BIOCHEMISTRY
including biophysical chemistry & molecular biology

Article

pubs.acs.org/biochemistry

FGF–FGFR Signaling Mediated through Glycosaminoglycans in Microtiter Plate and Cell-Based Microarray Platforms

Eric Sterner,[†] Luciana Meli,[†] Seok-Joon Kwon,[†] Jonathan S. Dordick,[†,‡,§,∥] and Robert J. Linhardt*[,†,‡,§,⊥]

[†]Department of Chemical and Biological Engineering, [‡]Department of Biomedical Engineering, [§]Department of Biology, [∥]Department of Material Sciences, and [⊥]Department of Chemistry and Chemical Biology, Center for Biotechnology and Interdisciplinary Studies, Rensselaer Polytechnic Institute, Troy, New York 12180, United States

Supporting Information

ABSTRACT: Fibroblast growth factor (FGF) signals cell growth through its interaction with a fibroblast growth factor receptor (FGFR) and a glycosaminoglycn (GAG) coreceptor. Here, we examine the signaling of five different FGFs (1, 2, 6, 8, and 8b) through FGFR3c. A small library of GAG and GAG-derivative coreceptors are screened to understand better the structure–activity relationship of these coreceptors on signaling. Initially, data were collected in a microtiter plate well-based cell proliferation assay. In an effort to reduce reagent requirements and improve assay throughput, a cell-based microarray platform was developed. In this cell-based microarray, FGFR3c-expressing cells were printed in alginate hydrogel droplets of ∼30 nL and incubated with FGF and GAG. Heparin was the most effective GAG coreceptor for all FGFs studied. Other GAGs, such as 2-*O*-desulfated heparin and chondroitin sulfate B, were also effective coreceptors. Signaling by FGF 8 and FGF 8b showed the widest tolerance for coreceptor structure. Finally, this on-chip cell-based microarray provides comparable data to a microtiter plate well-based assay, demonstrating that the coreceptor assay can be converted into a high-throughput assay.

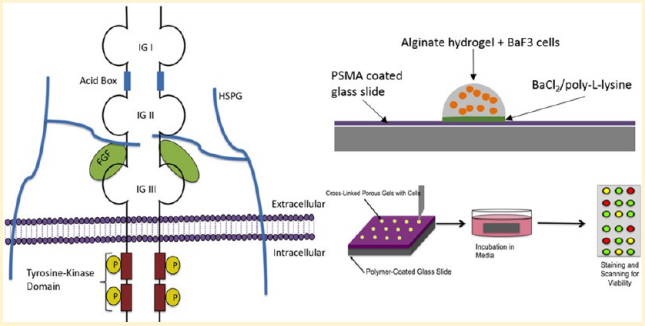

Glycosaminoglycans (GAGs) are a diverse family of linear, polyanionic polysaccharides possessing highly varied structural properties that dramatically affect their biological function.[1−4] GAG chains are found linked to a variety of core proteins, as proteoglycans (PGs),[5,6] and are localized primarily on the outer surface of eukaryotic cell membranes and in the extracellular matrix (ECM). Heparan sulfate (HS) and chondroitin sulfate (CS) are two structurally diverse families of GAGs that have been implicated in signaling. The major structural repeating units and the predominant sulfation patterns of each GAG and structurally modified GAG studied in this article are presented in Figure 1 and Table 1. HS is composed of a disaccharide unit of β-D-glucuronic acid (GlcA) or α-L-iduronic acid (IdoA) and a α-D-glucosamine residue (GlcN) in a repeating 1,4-glycosidic linkage. This HS disaccharide repeating unit often contains combinations of many different modifications, for example, sulfation of carbon-2 of IdoA or GlcA residues (IdoA2S or GlcA2S, where S is sulfo), sulfation of carbon-6 of a GlcN residue (GlcN6S), sulfation of carbon-3 of a GlcN residue (GlcN3S), and N acetylation or N sulfonation of a GlcN residue (GlcNAc or GlcNS, respectively, where Ac is acetyl). Heparin is a highly sulfated HS-type polysaccharide typically containing more than an average of 2.7 sulfo groups per disaccharide with a major subunit structure of IdoA2SGlcNS6S that contains three sulfo groups (Figure 1). CS is somewhat less complex, composed of a disaccharide unit of GlcA or IdoA and an α-D-*N*-acetylgalactosamine (GalNAc) in alternating 1,4-, 1,3-glycosidic linkages. CS can be modified with sulfation of carbon-4 or -6 of GalNAc and/or carbon-2 of GlcA or IdoA.

HS and CS polysaccharides are typically isolated from a variety of different animal tissues.[7−9] CS GAGs are typically derived from cartilage and have the major biological function of maintaining the structure of that tissue.[3,10,11] CS has pharmacological roles and is used as a nutraceutical to treat arthritis.[12] The major biological function of HS GAGs is the regulation of biological pathways, including growth factor signaling, chemokine chemotaxis, and coagulation/complement cascades, by binding to a variety of proteins, including growth factors such as fibroblast growth factors (FGFs) and Wnt, chemokines, such as interleukins, and coagulation proteins, such as antithrombin.[2,13−16] In FGF signaling, the HS GAG chain of the HSPG is considered a coreceptor and is generally crucial for efficient signaling of FGF through its protein-based receptor.[17] Heparin has a major pharmacological role as an anticoagulant drug.[18,19] Recently, the involvement of CS GAGs in the regulation of biological pathways has also been reported.[20]

Received: September 14, 2013
Revised: November 29, 2013
Published: November 29, 2013

   dx.doi.org/10.1021/bi401284r | *Biochemistry* 2013, 52, 9009−9019

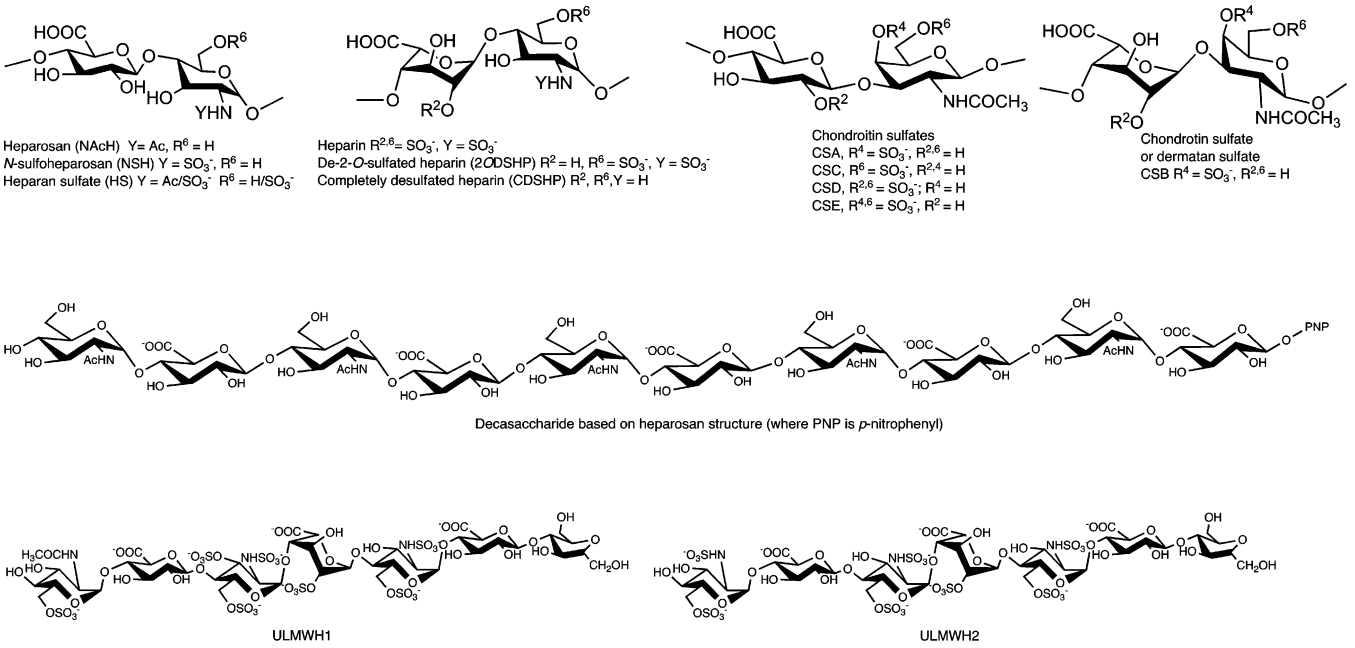

Figure 1. Major disaccharide-repeating units of heparin, HS, NAcH, NSH, and CS-type glycosaminoglycans shown together with the structures of decasaccharide, ULMWH1, and ULMWH2. Note that heparin HS, NSH, and CS-type glycosaminoglycan chains also typically contain many other minor structures (e.g., heparin contains GlcNAc and GlcA residues with and without C-2 *O*-sulfo groups as well as glucosamine residues without C-6 without *O*-sulfo groups and with C-3 *O*-sulfo groups).

Table 1. Major Sulfation Patterns and Iduronic Acid Content of HS-Type and CS-Type GAGs Tested in Combination with FGFR3c and Multiple FGFs

name	N substitution	iduronic acid	2S	6S	3S
heparosan (NAcH)	Ac	−	−	−	−
N-sulfo heparosan (NSH)	SO_3^-	−	−	−	−
heparan sulfate	Ac/SO_3^-	−/+	−/+	−/+	−/+
completely desulfated heparin (CDSHP)	H	+	−	−	−
2-*O*-desulfated heparin (2ODSHP)	SO_3^-	+	−	+	−/+
heparin	SO_3^-	+	+	+	−/+
			2S	4S	6S
chondroitin sulfate A (CSA)	Ac	−	−	+	−
chondroitin sulfate B (CSB)	Ac	+	−	+	−
chondroitin sulfate C (CSC)	Ac	−	−	−	+
chondroitin sulfate D (CSD)	Ac	−	+	−	+
chondroitin sulfate E (CSE)	Ac	−	−	+	+

The FGF family of proteins are a major class of signaling proteins.[21] In humans, the 22 FGFs are responsible for a variety of cellular functions, including proliferation, differentiation, and angiogenesis.[22,23] These FGFs show varying selectivity and affinity for binding to FGF receptors (FGFRs), with some FGFs exhibiting extremely strong (nanomolar) binding to multiple FGFRs and some FGFs showing no binding to any FGFR.[24,25] There are four different cell-surface-bound FGFRs (1−4) with FGFRs 1, 2, and 3 exhibiting b and c splice variants and FGFR 4 exhibiting a Δ splice variant, comprising a total 7 unique FGFRs.[26]

A substantial amount of research has been dedicated to understanding the interactions of FGFs and FGFRs with HSPGs.[24,25,27−29] This research has most commonly employed affinity chromatography or surface plasmon resonance (SPR) to evaluate relative FGF, FGFR, and HS binding affinities.[21,27,28,30] These techniques, however, measure only binding and lack important biological information on the ability of the binary or ternary complexes formed to initiate FGF signaling pathways.

Biological studies on the ability of FGF−FGFR−HS ternary complexes (Figure 2A) to initiate FGF signaling pathways are most commonly performed using cell-based proliferation assays that employ immortalized murine bone marrow (BaF3) cells that express a single FGFR and no HSPG on the cellular surface.[24,25] These studies have primarily been used to evaluate the interaction and signaling by full-length heparin (~10−12 kDa) of various combinations of FGFs and FGFRs.[17] Studies have also been performed that evaluate both the potential of smaller enzymatically derived heparin derivatives (dp 2−20) or variably chemically desulfated heparins,[31,32] but these studies tend to be limited to only a few FGFs and have often afforded conflicting results.[17,33,34]

The development of a high-throughput, miniaturized bioassay would be extremely beneficial for testing the overwhelming number of combinations of FGF, FGFR, and GAG available for experimentation. Currently, there is precedent for

dx.doi.org/10.1021/bi401284r | *Biochemistry* 2013, 52, 9009−9019

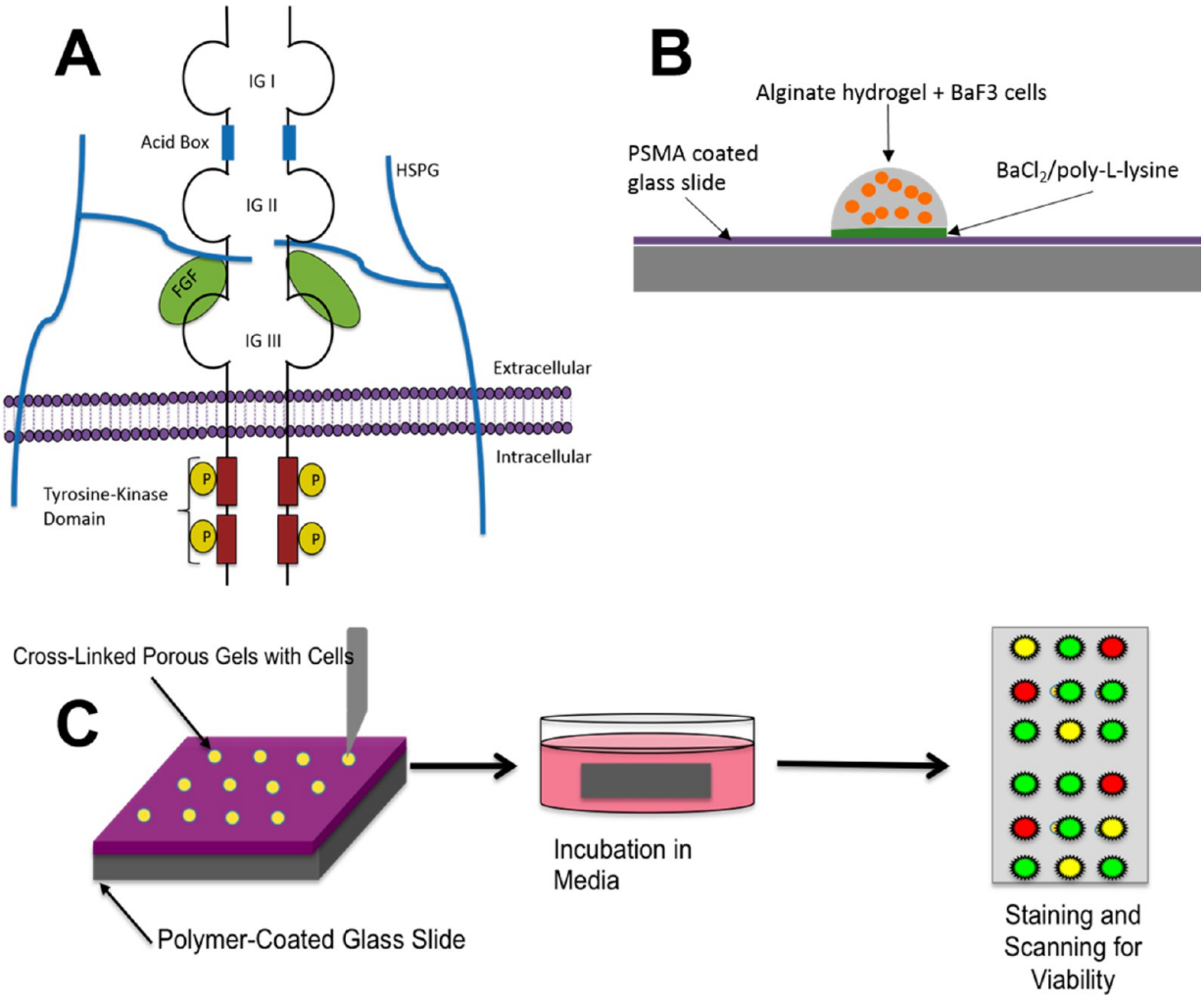

Figure 2. Mechanism of FGF−FGFR−GAG signal transduction and methods to measure this activity. (A) Ternary complex assembly of fibroblast growth factor (FGF), fibroblast growth factor receptor (FGFR), and surface-bound heparan sulfate proteoglycan (HSPG). In the case of BaF3 cells, the surface of the cell is devoid of HSPGs, and HS-type or CS-type GAGs can be added in combination to mediate the formation of the ternary complex and initiate cellular proliferation. (B) Outline of the procedure to microarray cells. Acid-washed glass slides are first coated with 0.1% polystyrene comalic anhydride (PSMA) and dried overnight. Next, a solution of $BaCl_2$ and poly-L-lysine (PLL) is arrayed to the slide and dried. Finally, the viscous solution of 1% alginate with BaF33c cells is arrayed on top of the dried $BaCl_2$:PLL spots. Appropriate media solutions are added to the slide and are incubated at 37 °C and 5% CO_2. (C) Following incubation, the slides are live/dead stained with calcein AM and ethidium homodimer and left to dry. The dried slides are scanned to measure cellular proliferation.

the application of high-throughput 3D cell-assay platforms, which have been used successfully for stem cell differentiation, on-chip immunofluorence, and cytotoxicity assays.[35−37] These 3D platforms, however, have not been extended to bioassays specifically involving growth factor signaling. Because 2D array-based platforms have been successfully developed for heparin glycan−FGF 2 screening,[38] we decided to examine how 3D chip platforms would perform in such applications.

Herein, we examine the specific structure(s) within HS and CS GAGs that are important for forming FGF−FGFR−GAG ternary complexes capable of promoting BaF3 cellular proliferation. A small library of HS polysaccharides and oligosaccharides, heparin derivatives, and CS polysaccharides of various molecular weights and sulfation levels and sulfation patterns was tested against FGFs 1, 2, 6, 7, 8, and 8b with a BaF3 cell line expressing FGFR3c in a pseudo 3D, 96-well plate environment. These studies utilized defined concentrations of FGF and GAG to provide an experimental baseline for determining BaF3 cellular proliferation. Finally, these GAGs and FGFs were retested against the BaF3 cell line on the high-throughput, miniaturized 3D chip platform for validation of both the methodology and consistent growth patterns.

EXPERIMENTAL PROCEDURES

Materials. Human recombinant FGF 1 and FGF 2 expressed in *Escherichia coli* were a gift from Amgen (Thousand Oaks, CA). Human recombinant FGF 6, FGF 7, FGF 8, and FGF 8b were purchased from Invitrogen Life Technologies (Carlsbad, CA). Heparin and HS, prepared from porcine intestine, were purchased from Celsus Laboratories Inc. (Cincinnati, OH). Heparosan (NAcH) was prepared from the *E. coli* K5 strain by fermentation of glucose and ammonium chloride.[39] *N*-Sulfoheparosan (NSH) was prepared by the chemical de-N-acetylation/N-sulfation of heparin.[40] Chemically de-2-*O*-sulfated heparin (2ODSHP) was prepared as described in the literature.[41] Completely desulfated HP (CDSHP) was prepared as described in the literature.[42] CS type A (CSA), from bovine trachea, CSC, from bovine cartilage, CSD, from

dx.doi.org/10.1021/bi401284r | *Biochemistry* 2013, 52, 9009−9019

shark cartilage, and CSE, from squid cartilage, were purchased from Sigma-Aldrich (St. Louis, MO). CSB (also known as dermatan sulfate), from porcine intestinal tissue, was purchased from Celsus. The BaF3 cell line used in this study was a generous gift from David Ornitz of Washington University, St. Louis, MO.

BaF3 Cell Culture. Immortalized murine bone marrow cells expressing the FGFR3c (designated BaF33c)[24,43] were maintained in RPMI 1640 with L-glutamine media supplemented with 10% fetal bovine serum (FBS), penicillin–streptomycin, and β-mercaptoethanol. Geneticin (G418) and interleukin-3 were added to concentrations of 400 μg/mL and 1 ng/mL, respectively. These cells were maintained at 37 °C and 5% CO_2 in sterile, polycarbonate Erlenmeyer flasks, with continuous shaking at 125 rpm. Cells were routinely passaged every 3 days and reseeded at 200 000 cells per milliliter.

Ninety-Six-Well Plate Proliferation Assays. Prior to experimentation with FGFs, the FGFR-expressing BaF3 cells were counted using a hemacytometer and pelleted by centrifugation at 200 rcf for 5 min. The media was removed by vacuum aspiration, and the cells were washed with interleukin-deficient RPMI media. The cells were then centrifuged and washed an additional three or four times. After the final centrifugation, the cells were resuspended in RPMI media containing 10% FBS, penicillin–streptomycin, β-mercaptoethanol, and Geneticin. No interleukin-3 was added for these bioassays. The BaF3 cells were then added to a clear, U-bottomed 96-well plate at a concentration of approximately 10 000 cells per well. Different FGFs were then added to the BaF3 cell-containing wells to a final concentration of 20 nM followed immediately by the addition of the different HS or CS polysaccharide being tested to a final concentration of 4.9 μg/mL and a total well volume of approximately 100 μL. Each 96-well plate was covered with a breathable membrane (Sigma) that allows for oxygen and CO_2 transfer but inhibits evaporation from the low-volume wells. The 96-well plates were then placed on a 125 rpm shaker in a 37 °C and 5% CO_2 incubator for 48 h.

After 48 h, the 96-well plates were removed from the incubator, the breathable membranes were removed, and the number of cells per well was analyzed using MTT assay. Briefly, 100 μL of 2.5 mg/mL thiazolyl blue tetrazolium bromide (Sigma) was added to each well, and the plate was incubated at 37 °C under 5% CO_2 for 3 h. The 96-well plate was then centrifuged for 10 min at 200 rcf to settle the formazan crystals at the bottom of each well. The solution in each well was carefully removed using a multichannel pipet and replaced with 150 μL of dimethyl sulfoxide (DMSO). The 96-well plate was gently shaken for 45 min to dissolve the crystals. Plates were then analyzed using a Molecular Devices (Sunnyvale, CA) SpectraMax M5 microtiter plate reader at 590 and 690 nm.

Three-Dimensional Chip-Based Proliferation. Prior to printing the BaF3 cell on the microchip surface, the cells were pelleted at 200 rcf and washed with interleukin-3-deficient RPMI media five times in a manner identical to the method used for the 96-well plate assay. Following the final washing step, the cells were resuspended at 5×10^6 cells per milliliter in RPMI media supplemented with 10% FBS, penicillin–streptomycin, β-mercaptoethanol, and G418.

Poly(styrene comalic anhydride) (PSMA) was dissolved in toluene at 1% (w/v). Once the PSMA was completely dissolved, the solution was further diluted to 0.1% (w/v). The 0.1% PSMA solution was then spin-coated onto the acid-washed microscope slides using a Laurell Technologies (North Wales, PA) WS-400B spin-coater. The coated slides were left to dry overnight.

A 30 nL solution of a 0.1 mM $BaCl_2$:poly-L-lysine (1:2) was spotted onto PSMA-coated slides using a MicroSys 5100-4SQ noncontact microarray spotter (Genomic Solutions, now Digilab, Inc., Marlborough, MA) and left to dry for approximately 1 h. Briefly, this microarray-based approach employs pump-based aspiration and dispensing through a 100 μm ceramic tip with high positional accuracy. For these experiments, the $BaCl_2$:poly-L-lysine solution was arrayed in a 2 × 4 block pattern, with each block containing a 6 × 8 array of individual spots.

Next, BaF3 cells in RPMI media deficient of interleukin-3 were mixed with a 3% alginate solution at a 2:1 ratio (Figure 2B, 2C). Cell/alginate solution (30 nL) was arrayed onto each dried $BaCl_2$/PLL spots under humidified conditions. The spots were incubated for 2 min to complete the formation of a stable cross-linked alginate hydrogel. The conditions were set so that each 30 nL spot contained approximately 100 cells prior to incubation. The resulting 30 nL cell-containing alginate-hydrogel spot was approximately 580 nm in diameter and 150 nm in height, similar to that previously described in the literature.[37]

An 8-well, polystyrene medium chamber (Nunc Lab-Tek II) was applied over the slide to compartmentalize individual sets of conditions. One hundred microliters of RPMI media (supplemented with 10% FBS, penicillin–streptomycin, β-mercaptoethanol, and G418) was added to each chamber. The RPMI media also contained FGF and HS or CS-GAGs at concentrations consistent with the 96-well plate concentrations. A breathable membrane was applied over the chamber, and the slide was incubated at 37 °C and 5% CO_2 for 48 h.

Following incubation, the breathable membrane was discarded, and the media was removed. The 8-well chamber was removed, and the slide was washed by submersion in 20 mM $CaCl_2$ and 140 mM NaCl (pH 7.0) buffer for 5 min. This washing step was repeated an additional two times with fresh $CaCl_2$ and NaCl solution. Following the washes, the slide was stained with a calcein AM/ethidium homodimer live/dead assay kit (Life Technologies) for 45 min. The staining of the slides was followed by two additional 15 min washes with $CaCl_2$ and NaCl solution. Finally, the slide was left to dry overnight in the dark.

Live/dead assessment of the dried slides was completed using a Genepix Professional 4200 (Molecular Devices) slide scanner with a blue laser (488 nm) with a standard blue filter and a 645AF75/594 filter for the green and red dyes, respectively. The green and red fluorescence intensity was quantified using GenePix Pro 6.0 software (Molecular Devices).

Interleukin-Mediated On-Chip Growth. Additional 3D chips were printed in a method identical to that previously described to validate that cells grow in an identical manner on-chip as they do in a shaker flask. In these experiments, instead of the application of the 8-well chamber to the chip and the addition of FGF/GAG-supplemented media to the well, these chips were submerged in 5 mL of RPMI media containing 1 ng/mL interleukin-3. At time points of 0, 29, 48, and 56 h, one slide was removed from incubation, washed, live/dead-stained, and dried in a procedure identical to the method previously described.

Data Analysis. The data were analyzed in a method similar to previous studies involving FGF, FGFR3c, and HP

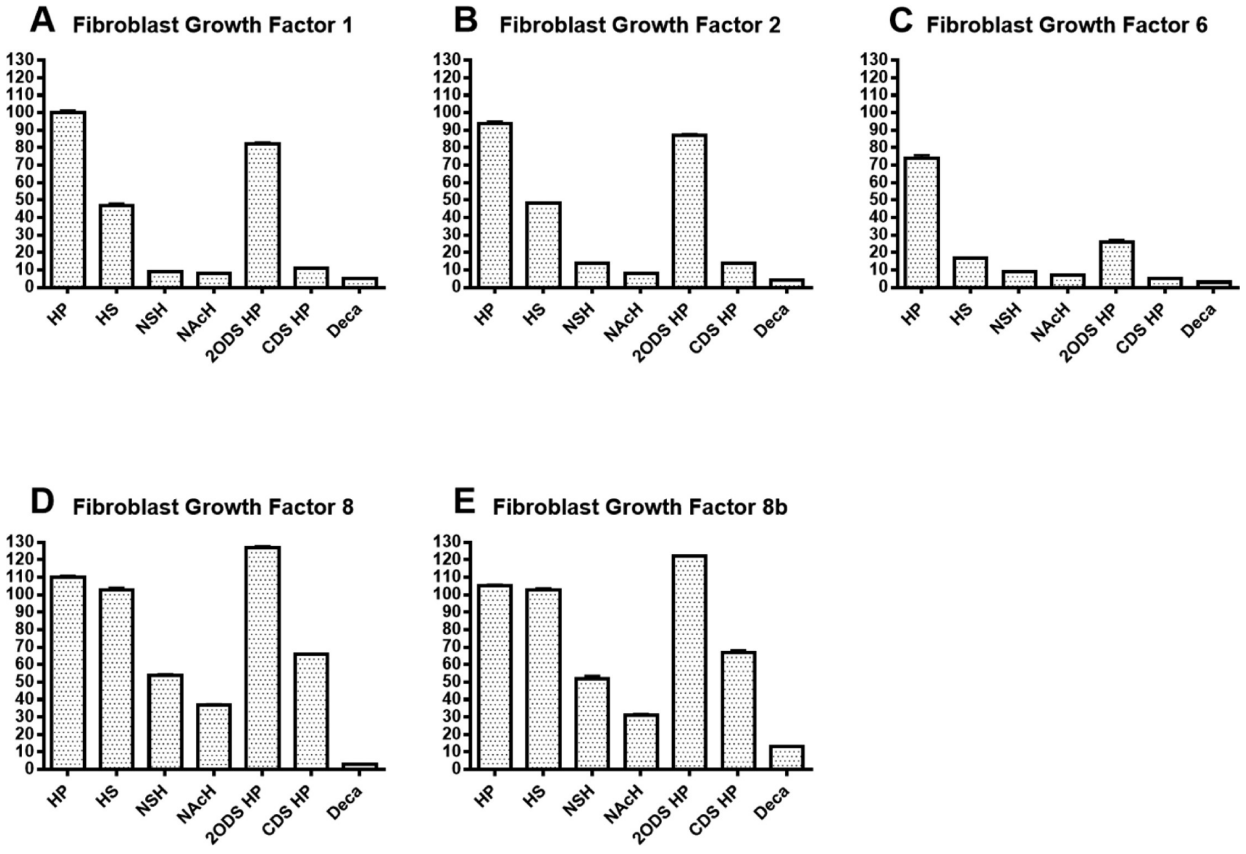

Figure 3. Results from a 96-well plate assay of combinations of HS-type GAGs with FGFs and FGFR3c. Each of the five graphs is representative of an individual FGF tested across seven unique HS-type GAGs. Each FGF−GAG combination was tested in eight replicates to confirm assay accuracy and repeatability. Following incubation, plates were assayed for cell viability using a standard MTT assay. All cellular proliferation percentages are relative to the FGF 1−heparin positive control (100%). Panels A−E show FGF 1, FGF 2, FGF 6, FGF 8, and FGF 8b, respectively.

Table 2. Relative Cellular Proliferation Extents for the HS-Type and CS-Type GAGs Tested

	fibroblast growth factor ligand				
fibroblast growth factor receptor (FGFR3c)	FGF 1 ± SE (%)	FGF 2 ± SE (%)	FGF 6 ± SE (%)	FGF 8 ± SE (%)	FGF 8b ± SE (%)
Heparan Sulfate Glycosaminoglycans					
heparin (HP)	100 ± 3	94 ± 2	74 ± 4	110 ± 2	105 ± 1
heparan sulfate (HS)	47 ± 2	48 ± 1	17 ± 1	103 ± 2	103 ± 2
N-sulfoheparosan (NSH)	9 ± 1	14 ± 1	9 ± 1	54 ± 2	52 ± 3
heparosan (NAcH)	8 ± 1	8 ± 1	7 ± 1	37 ± 2	31 ± 2
2-O desulfated heparin (2*O*DSHP)	82 ± 2	87 ± 2	26 ± 2	127 ± 3	122 ± 2
completely desulfated heparin (CDSHP)	11 ± 1	14 ± 1	5 ± 1	66 ± 2	67 ± 2
unmodified decamer (Deca)	5 ± 1	4 ± 1	3 ± 1	3 ± 0	13 ± 1
Chondroitin Sulfate Glycosaminoglycans					
chondroitin sulfate A (CSA)	2 ± 0	6 ± 0	4 ± 0	34 ± 0	29 ± 2
chondroitin sulfate B (CSB)	62 ± 1	74 ± 1	17 ± 1	98 ± 2	98 ± 2
chondroitin sulfate C (CSC)	0 ± 0	2 ± 0	0 ± 0	46 ± 1	32 ± 3
chondroitin sulfate D (CSD)	0 ± 0	1 ± 0	2 ± 0	45 ± 1	41 ± 3
chondroitin sulfate E (CSE)	13 ± 0	34 ± 3	3 ± 0	47 ± 1	47 ± 5

interactions in an effort to consistently compare the results of each polysaccharide and fibroblast growth factor combination across the entire data set. The extent of proliferation observed with heparin and FGF 1 was set at 100% to represent an arbitrary maximal cellular proliferation. For each FGF and FGFR3c interaction, a negative control involving the addition of FGF in the absence of GAG was used for zero growth. Each combination of GAG and FGF was then compared against the internal zero growth control and the arbitrary FGF 1−heparin value to determine relative cellular proliferation.

RESULTS AND DISCUSSION

Heparan Sulfate Polysaccharides. Fibroblast growth factors 1, 2, 6, 8, and 8b at a solution concentration of 20 nM were probed for their BaF3 cell proliferative activities in the presence of heparin (Figure 3 and Table 2) to confirm that the assay system was functioning. The arbitrary maximum, FGF 1 with heparin (Figure 3A), demonstrated excellent proliferative activity and was used for comparison. FGF 2 also demonstrated excellent heparin-mediated FGFR3c cell proliferative ability

dx.doi.org/10.1021/bi401284r | *Biochemistry* 2013, 52, 9009−9019

(Figure 3B), comparable to FGF 1, consistent with previously published data.[24,25,43] Additionally, heparin had moderate, approximately 75% of the arbitrary maximum, ability to induce BaF3 cell proliferation with FGF 6 (Figure 3C), also consistent with literature.[25] However, slight inconsistencies were observed when comparing the HP-mediated FGFR3c cell proliferative activity of FGF 1, FGF 8, and FGF 8b (Figure 3, panels D and E, respectively). FGF 1, FGF 8, and FGF 8b showed nearly identical cell proliferation over the 48 h incubation period, with the FGF 8 and 8b promoting 10 and 5% more growth, respectively. Previous studies demonstrated that FGF 8 showed approximately half of the maximal cell growth of FGF 1 in combination with heparin and FGFR3c over similar incubation times.[25] The differences between the current study and previously published data might be explained by the differences in solution concentrations of the FGFs, as the current studies use 4- to 8-fold higher growth factor concentrations to obtain optimal concentration-based proliferation for BaF3 cell growth. Our decision to work at slightly higher FGF and GAG solution concentrations was determined by preliminary dose-response analysis using HP, HS, and NSH with FGF 1 and 2 (Figures S1 and S2). At 10 nM solution concentrations of FGF 1 and FGF 2 (Figure S3), HP was capable of promoting cellular proliferation, but HS and other nonsulfated HS GAGs were not. By performing a simple preliminary dose-response curve, the abilities of HS and NSH improved with increasing FGF concentration (Figure S1). We also found that changing the GAG concentrations did not benefit cellular proliferation (Figure S2). Although FGF conditions could have been tested as high as 160 nM, we compromised by using a solution concentration of 20 nM in all experiments.

After demonstrating that heparin and the selected FGFs induced cellular growth levels consistent with the literature, HS and modified heparins were next examined to understand better the structure−activity relationship of FGF−FGFR−GAG signaling. Two GAGs of particular interest were selected with a reduced level of sulfation, HS and 2*O*DSHP (Figure 1 and Table 1). Porcine intestinal HS is primarily composed of GlcA (>60% of total uronic acid[45]) and has very low levels of 2-sulfo group-modified uronic acid (<13% of total uronic acid[44,45]), with its sulfo groups carried primarily by the GlcN residue as either GlcNS, GlcNAc6S, or GlcNS6S (29−38, 7−10, and 5−8%, respectively, corresponding to ≤1 sulfo group/disaccharide repeating unit.)[44] 2*O*DSHP is primarily composed of IdoA (>70% of total uronic acid),[41] with its sulfo groups carried entirely by GlcN residue as either GlcNS, GlcNAc6S, or GlcNS6S (1−3,1−3, and >80%, respectively, corresponding to ∼1.7 sulfo groups/disaccharide)[41,45] and is identical to heparin except that it lacks 2-sulfo uronic acid residues.

A final set of GAGs, of particular interest in our study, is a set that possess low-to-no sulfation as well as GAGs of low molecular weight. NAcH was our first choice because it has a high molecular weight but no sulfo groups (Figure 1 and Table 1). NAcH is entirely composed of repeating GlcA and GlcNAc residues for a M_n that typically ranges between 20 000 and 50 000. *N*-Sulfoheparosan (NSH), another low sulfation GAG, is an intermediate in heparin biosynthesis. In the case of NSH, the disaccharide repeating unit is composed of a GlcA residue followed by a GlcN residue as either GlcNS or GlcNAc (85 and 15%, respectively). NSH is prepared from NAcH by base-catalyzed de-N-acetylation followed by chemical N sulfonation in a process that results in a GAG with reduced molecular weight, M_w ∼11.2 kDa.[40] Chemically modified heparins were also tested. Completely desulfated heparin (CDSHP) was chosen as a GAG that possesses no sulfo groups but is still composed primarily of iduronic acid residues (IdoA and GlcA of 80 and 20%, respectively). An unsulfated HS decasaccharide (Deca) of M_w 3.1 kDa with a NAcH repeating structure of GlcA and GlcNAc (Figure 1) was examined to determine whether such a minimal structure could promote FGF−FGFR binding and signaling.

Using this small library of HS GAGs, including HS, NSH (∼1 sulfo group/disaccharide), NAcH (0 sulfo groups/disaccharide), 2*O*DSHP (∼1.7 sulfo groups/disaccharide), CDSHP (0 sulfo groups/disaccharide), and Deca (0 sulfo groups/disaccharide), FGF signaling was examined in the BaF3 assay. Under treatment with FGF 1 and FGF 2 (Figure 3A,B), 2*O*DSHP was the best promoter of proliferation, showing activity most comparable to the heparin positive control. The relative proliferation levels of 2*O*DSHP with FGF 1 and FGF 2 were 82 and 87% of that of heparin (Table 2). Although HS showed substantially lower activity than heparin and 2*O*DSHP, the level of FGF 1 and FGF 2 HS-activated cellular proliferation was approximately 50% (Table 2) of that of heparin. The remaining GAGs (NSH, NAcH, CDSHP, and Deca) tested in combination with FGF 1 and FGF 2 were incapable of promoting levels of proliferation greater than 15% (Table 2). These data suggest that FGF 1 and FGF 2 prefer HS GAGs with a high level of sulfation and a high IdoA content to signal through FGFR3c.

When the same HS GAGs were tested in combination with FGF 6 (Figure 3C), very low overall levels of FGFR3c-induced proliferation were observed. It is also noteworthy that the FGFR3c level of proliferation of heparin with FGF 6 was reduced as compared to heparin with FGF 1. 2*O*DSHP showed modest activity (26%) with FGF 6 but much less activity than that observed with FGF 1 (82%) and FGF 2 (87%). The removal of the 2-sulfo groups resulted in >60% reduction in FGF 6-induced proliferation levels, whereas for FGF 1- and FGF 2-induced proliferation, the reduction was ∼20%. HS-induced proliferation with FGF 6 was only 17% of that observed with heparin, and all other HS GAGs tested showed <10% BaF3 cell proliferation (Table 2).

Next, FGF 8- and FGF 8b-induced proliferation was examined (Figure 3D,E). These growth factors demonstrated the lowest levels of GAG specificity for cellular proliferation. Remarkably, 2*O*DSHP showed greater activity (127 and 122%, respectively) for FGF 8- and FGF 8b-induced proliferation of BaF3 cells than the arbitrary FGF 1−heparin control or the FGF 8− and FGF 8b−heparin experiments (Table 2). HS induced FGF 8 and FGF 8b proliferation levels comparable to heparin. CDSHP was also capable of promoting cell proliferation at 66 to 67% of the level of the heparin−FGF 1 positive control. NSH mediated FGF 8 and FGF 8b proliferation at 54 and 52%, respectively. Even NAcH, without sulfation, was a modest promoter of FGF 8 and FGF 8b cellular proliferation, at 37 and 31%, respectively. Unmodified decasaccharide showed low but detectable levels of cellular proliferation for both FGF 8 and FGF 8b. These data demonstrate that although sulfation increases cellular proliferation levels, the presence of sulfo groups are not a requirement for FGF 8- and FGF 8b-mediated proliferation of BaF3 cells. The low activity for the decasaccharide, however, clearly suggests a length requirement for nonsulfated polysaccharide-based signaling involving FGF 8 and FGF 8b.

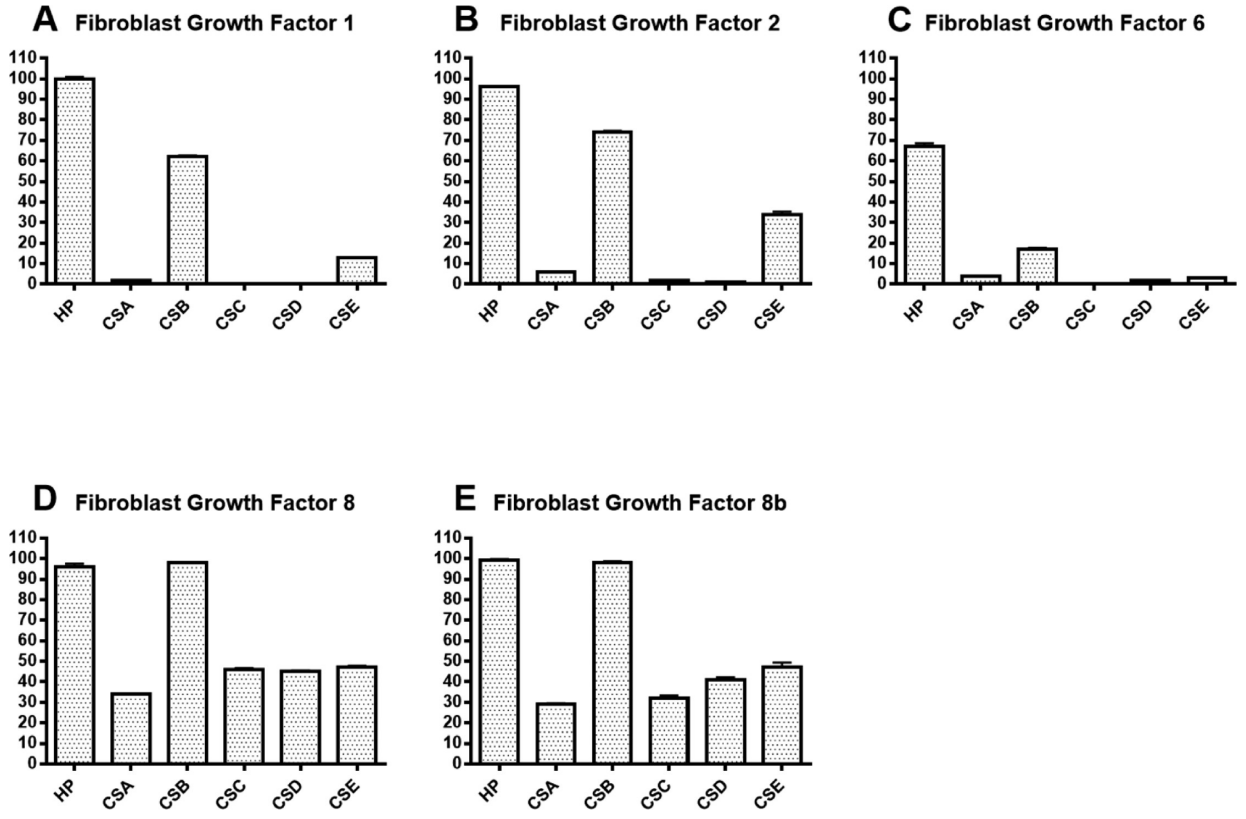

Figure 4. Results from a 96-well plate assay of combinations of CS-type GAGs with FGFs and FGFR3c. Each of the five graphs is representative of an individual FGF tested across five unique CS-like GAGs. Each FGF−GAG combination was tested in eight replicates to confirm assay accuracy and repeatability. Following incubation, plates were assayed for cell viability using a standard MTT assay. All cellular proliferation percentages are relative to the FGF 1−heparin positive control (100%). Panels A−E show FGF 1, FGF 2, FGF 6, FGF 8, and FGF 8b, respectively.

Chondroitin Sulfate Polysaccharides. The five CS-type GAGs studied represent a natural library of structurally diverse molecules (Figure 1 and Table 1). CSA, CSB, and CSC contain ∼1 sulfate per disaccharide repeating unit. In CSA and CSB, this sulfo group is located at carbon-4 of the galactosamine residue, and in CSC, it is located at carbon-6 of the galactosamine residue. CSB, commonly referred to as dermatan sulfate, differs from CSA in that it contains an iduronic acid in place of glucuronic acid. Thus, CSB more closely resembles heparin and chemically modified heparin derivatives. CSD and CSE both have ∼2 sulfates per disaccharide repeating unit. CSD has sulfates at carbon-2 and carbon-6 of the *N*-acetyl galactosamine residue. CSE has sulfates at carbon-2 and carbon-6 of the *N*-acetyl galactosamine residue.

CSB and CSE in combination with FGF 1 and FGF 2 (Figure 4A,B) were capable of promoting the proliferation levels by 10−75% (Table 2) of that of the heparin-containing positive control. When CSA, CSC, and CSD were examined with FGF 1, FGF 2, and FGF 6, they were all poor promoters of BaF3 cell proliferation (Figure 4A−C), with <6% of the activity of the heparin-containing positive control. Only CSB showed activity in promoting FGF 6-induced cell growth (Figure 4C and Table 2).

Experiments on FGF 8 and FGF 8b (Figure 4D,E and Table 2) again showed the lowest specificity for CS GAG-mediated promotion of cellular proliferation, in a manner similar to the HS-GAG-mediated experiments. CSB displayed levels of proliferation comparable to the heparin control. CSC, CSD, and CSE all promoted similar extents of proliferation (45−47%) with FGF 8 (Figure 4D), whereas the extent to which CSA promoted proliferation was slightly lower (34%). In combination with FGF 8b (Figure 4E), CSD- and CSE-mediated proliferation were very similar (41−47%), and CSA demonstrated similar levels of proliferation to CSC (29−32%).

On the basis of the surprising levels of proliferation mediated by CSB and CSE, we chose to explore a simple FGF dose-response curve on the 96-well plate platform for CSB−FGF 2 and CSE−FGF 2 (Figure 5). In these experiments, FGF 2 levels were varied between 0 and 320 nM. The half-maximal concentrations for CSB and CSE were 5.6 and 10.1 nM, respectively. Heparin showed a half-maximal value of 2.5 nM.

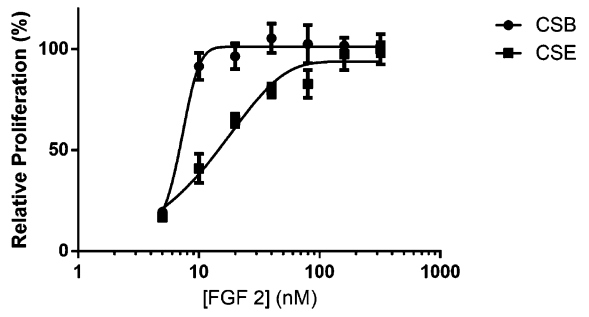

Figure 5. Half-maximal growth curve of chondroitin sulfate B (CSB) and chondroitin sulfate E (CSE) with FGF 2. Experiments were run in a 96-well plate, and samples were assayed for cell viability using a standard MTT assay. FGF 2 concentrations were varied from 0 to 320 nM in solution and run in eight replicates. CS-GAG concentrations were held constant at 4.9 μg/mL.

dx.doi.org/10.1021/bi401284r | *Biochemistry* 2013, 52, 9009−9019

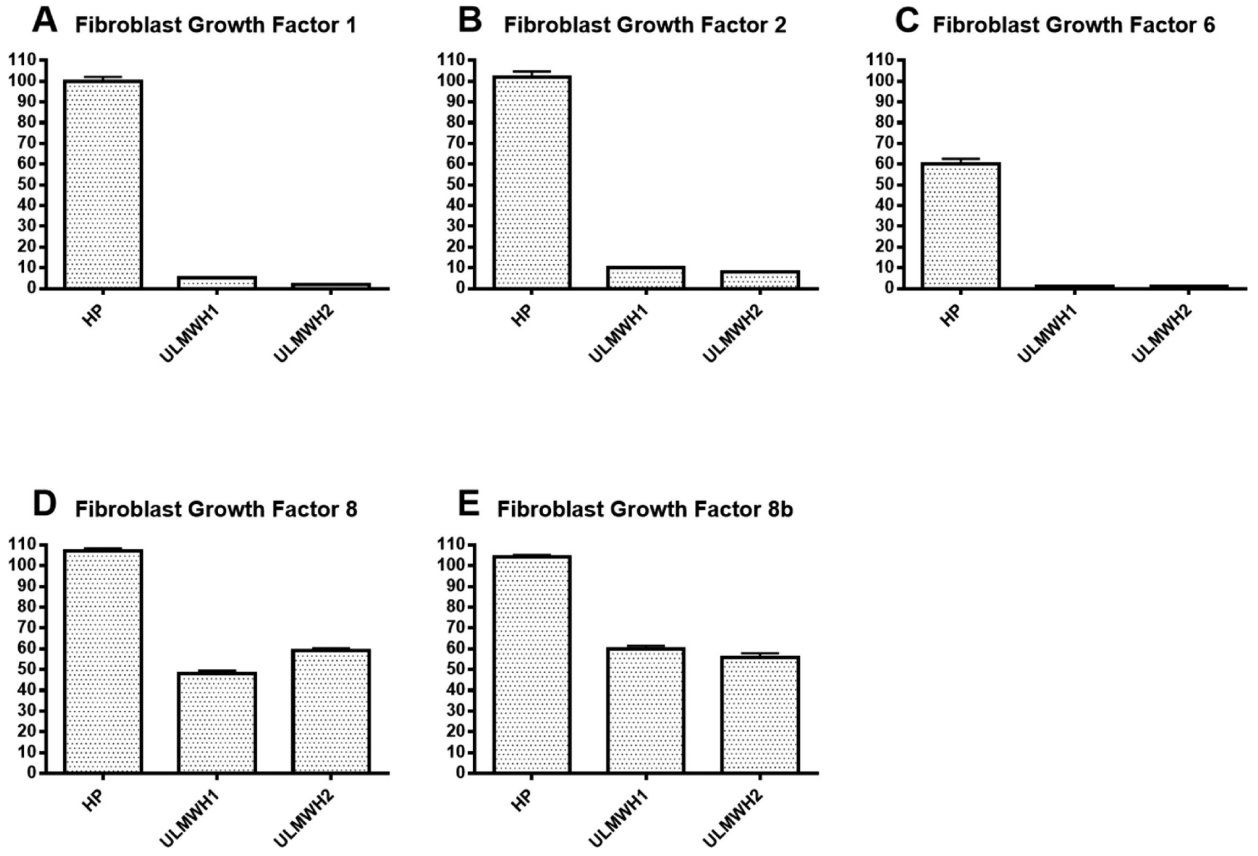

Figure 6. Results from a 96-well plate assay of combinations of ultra-low-molecular-weight heparins (ULMWHs) with FGFs and FGFR3c. Each FGF-GAG combination was tested in eight replicates to confirm assay accuracy and repeatability. Following incubation, plates were assayed for cell viability using a standard MTT assay. All cellular proliferation percentages are relative to the FGF 1−heparin positive control (100%). Panels A−E show FGF 1, FGF 2, FGF 6, FGF 8, and FGF 8b, respectively.

These results afford interesting information on the structure−activity relationship for optimal for cellular proliferation. On the basis of the proliferation patterns observed for the HS-GAGs (Figure 3), our expectation was that higher levels of sulfation were the primary driving force behind FGF−GAG−FGFR interaction and subsequent proliferation. This is primarily supported by Figure 3A−C, where HP, HS, and 2*O*DSHP are substantially better promoters of proliferation than their desulfated counterparts, NSH, NAcH, and CDSHP. However, investigation of the CS-GAGs seems to alter this prediction. Robust FGF 2 signaling for CSB (Figure 4), having IdoA but only ∼1 sulfo group per disaccharide, suggests an important role for IdoA in FGF 2-induced cell proliferation. Additional experiments will be required to understand fully the optimal balance between IdoA and sulfate content.

Ultra-Low-Molecular-Weight Heparins. Two ultra-low-molecular-weight heparins (ULMWH1 and ULMWH2) were next examined (Figures 1 and 6). These HS homogeneous heptasaccharides were prepared using chemoenzymatic synthesis.[46] The unnatural reducing terminal disaccharide of both ULMWHs was required for the initiation of chemoenzymatic synthesis. The last five residues of ULMWH1 are identical to the major antithrombin pentasaccharide-binding site in pharmaceutical heparin. The last five residues of ULMWH2 are identical to the antithrombin pentasaccharide-binding site in the drug Arixtra. ULMWH1 differed from ULMWH2 in the replacement of the nonreducing and glucosamine residue, GlcNS in ULMWH2 and GlcNAc in ULMWH1.

In combination with FGF 1, FGF 2, and FGF 6, ULMWH1 and ULMWH2 were incapable of promoting substantial levels of BaF3 proliferation (Figure 6). The low levels of proliferation observed with FGF 1 and FGF 2 are likely the result of the limited chain length rather than the extent of sulfation. Literature reports indicate that in the cases of FGF 1 and FGF 2 the most effective binding is seen at HS oligosaccharides of eight residues in length or longer.[25] The absence of FGF 6-induced BaF3 cell proliferation by ULMWHs (Figure 6C) is consistent with the low activity observed for HS and modified heparins (Figure 3). FGF 8 and FGF 8b (Figure 6D & E) again showed less stringent requirements for BAF3 cell proliferation. Both ULMWHs promoted cellular proliferation to >50% of the level observed for heparin. Surprisingly and despite their short chain length, these ULMWHs were potent promoters of BaF3 cell growth.

On-Chip Results: Interleukin-3 Growth. After testing the small library of HS and CS GAGs in combination with various FGFs and FGFR3c in a microtiter plate, our focus shifted to improving assay throughput by moving to a 3D chip platform. This platform also decreases the amount of reagents required to assess activity. Cellular proliferation on the 3D chip platform was first compared to Erlenmeyer flask growth. Growth in the presence of interleukin-3 was monitored on-chip. The doubling time of the BaF3 cells expressing FGFR3c and grown in shake flasks has been reported to be ∼20−22 h.[24]

Four slides were printed with the BaF3 cells suspended in 3D in alginate to monitor the growth of the cells on chip in the presence of interleukin-3 (Figures 2 and 7). One slide was

dx.doi.org/10.1021/bi401284r | *Biochemistry* 2013, 52, 9009−9019

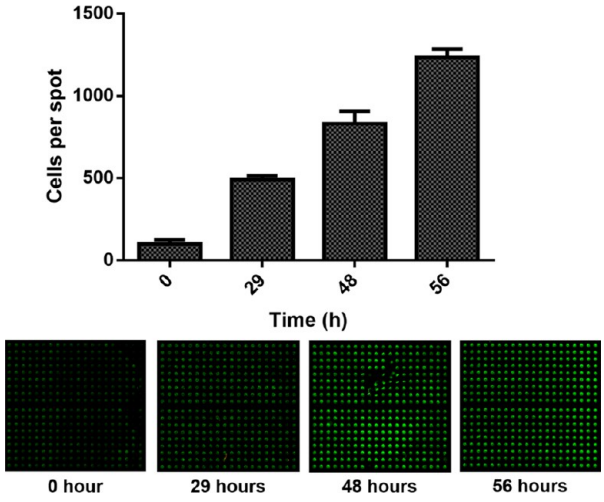

Figure 7. Measurement of on-chip growth of BaF33c cells in the presence of interleukin-3 as a mediator of growth over a 56 h period. Suspended in an alginate hydrogel, the cells appear to grow well with little cell death over this time period. Four slides were printed with BaF33c cells and incubated at 37 °C and 5% CO_2. At 0, 29, 48, and 56 h, a slide was removed from incubation, washed, and stained for cell viability. Cell viability was tested using a calcein AM/ethidium homodimer live/dead assay kit.

immediately stained with calcein AM and ethidium homodimer, dried, and scanned to determine the original cell density. The other three slides were submerged in RPMI 1640 media with G418 and 1 ng/mL of interleukin-3. At time intervals of 29, 48, and 56 h, the slides were removed from the RPMI 1640 media solution, washed with $CaCl_2$ and NaCl solution to eliminate residual media, and stained with calcein AM and ethidium homodimer. The slides were then dried overnight and scanned to determine the cell density within the alginate spots.

The BaF3 cells displayed continuous growth over a 56 h period with a small percentage of cell death (Figure 7). Starting at 100 cells per spot (3.3×10^6 cells/mL), the cells grew to over 1200 cells per spot (4.0×10^7 cells/SPH) at the 56 h time point. The doubling time of these cells in the 3D platform was calculated to be 16 h, slightly faster than the doubling time of the cells in the shake flasks.

On-Chip Results: HS-GAG- and CS-GAG-Mediated Growth. After the on-chip printing and cellular proliferation was confirmed in the presence of interleukin-3, HS- and CS-GAGs were next tested on the chip in combination with FGFs. These on-chip experiments were limited to FGF 1, FGF 6, and FGF 8 because these three FGFs provided a range of proliferation in the 96-well plate assay. FGF 1 was capable of promoting growth with highly sulfated, high IdoA content GAGs, but proliferation levels dropped for GAGs with low sulfation and low IdoA content (Figure 3A and Table 2). FGF 6 promoted lower levels of proliferation than FGF 1, regardless of the GAG examined, whereas FGF 8 again demonstrated the lowest specificity for GAG structure. Because only eight combinations can be tested on a single chip, our comparisons were made only between GAGs and a single type of FGF (Figure 8). Preliminary experiments were run to compare

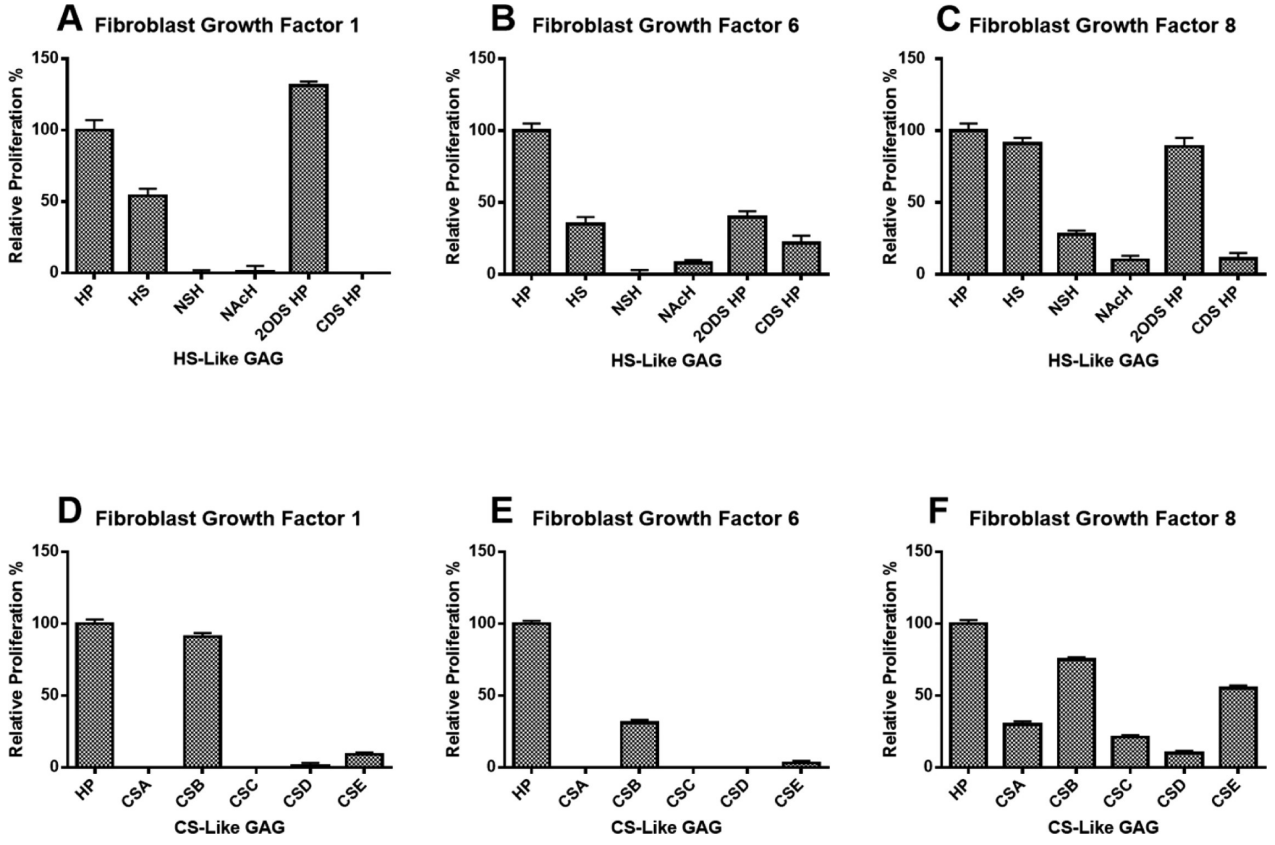

Figure 8. On-chip proliferation of BaF33c cells in combination with GAGs and FGFs. HS-type GAGs appearing in panels A–C are FGF 1, FGF 6, and FGF 8, respectively. CS-like GAGs appearing in panels D–F are FGF 1, FGF 6, and FGF 8, respectively. Forty-eight replicates can be tested on-chip with the same amount of solution required for one replicate on the 96-well plate platform.

dx.doi.org/10.1021/bi401284r | *Biochemistry* 2013, 52, 9009–9019

heparin−FGF-mediated cell growth to a GAG-deficient control in an effort to validate the 3D chip platform (Figure S4). Using a standard Student's t test, FGF 1- (Figure S4A), FGF 6- (Figure S4B), and FGF 8 (Figure S4C)-mediated cell growth were all significantly different ($p < 0.001$) and greater than their GAG-deficient controls.

The results of on-chip experiments closely matched those obtained in the microtiter plate. In the case of HS GAGs (Figure 8A−C), HS and 2*O*DSHP again were the most significant promoters of cellular proliferation as compared to the heparin control. In the cases of FGF 1 and FGF 6, the GAGs of low sulfation and low iduronic acid content again failed to promote cellular proliferation. In the case of FGF 8, the pattern again appeared showed HS and 2*O*DSHP to be significant promoters of cellular proliferation, with the other GAGs being low-to-moderate promoters. The only on-chip conditions where the FGF−GAG interaction did not closely match the microtiter plate experiments was in the case of CDSHP and FGF 8-mediated growth. Our expectation was for growth to be ∼67% of the positive control, but in these experiments growth was observed at ∼25% of the positive control (Figure 8C).

The results of the CS-like GAGs on-chip experiments (Figure 8D−F) also closely resembled the data previously obtained in microtiter plates. CSB continued to be the best promoter of BaF3 cell proliferation, relative to heparin, with all FGFs tested. CSE was the only other promoter of FGF 1 or FGF 6 cellular proliferation. In the case of FGF 8, all of the CS GAGs tested were capable of promoting BaF3 cellular proliferation, with CSB showing the highest activity.

Common FGF- and GAG-induced proliferation patterns were observed on both platforms, suggesting that the on-chip platform is a good candidate for the future development of high-throughput cell-based bioassays. Additionally, this platform allows for a substantial reduction in the overall material requirements for these bioassays. One block of 48 replicates requires less than 100 μL of solution, whereas 48 replicates in a 96-well plate would require over 5 mL of solution.

CONCLUSIONS

Highly sulfated HS-type GAGs, particularly ones with IdoA residues, were the best promoters of proliferation in all experiments. However, in the case of CS GAGs, the GAG showing the highest levels of proliferation was CSB, the only CS GAG containing iduronic acid residues. FGF 8 and FGF 8b displayed low specificity requirements for GAG-mediated promotion of cellular proliferation. ULMWHs showed little or no FGF 1, FGF 2, and FGF 6 promotion of BaF3 proliferation; however, these ULMWHs were capable of promoting proliferation through FGF 8 and FGF 8b.

The microarray platform outlined in this article represents a major step forward in the high-throughput study of growth factors, growth factor receptors, and GAGs. The microarray platform allows unique experiments, performed in replicates, that are required to study FGF and GAG combinations for just one FGFR. The development of this microarray-based platform also facilitates the testing of numerous combinations in parallel on a single chip and allows for an increased number of replicates and decreased amounts of reagent. Future work concerning this platform will involve making the platform more high-throughput to allow for hundreds of unique combinations to be performed in parallel with even more substantial reductions in material requirements.

ASSOCIATED CONTENT

Supporting Information

Dose-response data for FGF 2 and polysaccharides; comparison of polysaccharides for FGF signaling through FGFR; and statistical data validating the 3D microarray platform. This material is available free of charge via the Internet at http://pubs.acs.org.

AUTHOR INFORMATION

Corresponding Author

*Telephone: (518) 276-3404; Fax: (518) 276-3405; E-mail: linhar@rpi.edu.

Funding

This work was supported by grants from the National Institutes of Health (NIH): NIH GM38060, HL62244, and ES 020903.

Notes

The authors declare no competing financial interest.

ABBREVIATIONS USED

GAGs, glycosaminoglycans; FGF, fibroblast growth factor; FGFR, fibroblast growth factor receptor; ECM, extracellular matrix; HP, heparin; HS, heparan sulfate; NSH, *N*-sulfoheparosan; NAcH, heparosan; 2*O*DSHP, 2-*O*-desulfated heparin; CDSHP, completely desulfated heparin; Deca, unmodified decasaccharide; CS (A−E), chondroitin sulfate (A−E); ULMWH, ultra-low-molecular-weight heparin; IdoA, iduronic acid; GlcA, glucuronic acid

REFERENCES

(1) Esko, J. D., and Selleck, S. B. (2002) Order out of chaos: Assembly of ligand binding sites in heparan sulfate. *Annu. Rev. Biochem. 71*, 435−471.

(2) Capila, I., and Linhardt, R. J. (2002) Heparin-protein interactions. *Angew. Chem., Int. Ed. 41*, 391−412.

(3) Gallagher, J. T. (1989) The extended family of proteoglycans: Social residents of the pericelular zone. *Curr. Opin. Cell Biol. 1*, 1201−1218.

(4) Kreuger, J., Spillmann, D., Li, J.-P., and Lindahl, U. (2006) Interactions between heparan sulfate and proteins: The concept of specificity. *J. Cell Biol. 174*, 323−327.

(5) Ly, M., Laremore, T. N., and Linhardt, R. J. (2010) Proteoglycomics: Recent progress and future challenges. *OMICS 14*, 389−399.

(6) Cattaruzza, S., and Perris, R. (2006) Approaching the proteoglycome: Molecular interactions of proteoglycans and their functional output. *Macromol. Biosci. 6*, 667−680.

(7) Linhardt, R. J. (2003) Heparin: Structure and activity. *J. Med. Chem. 46*, 2551−2554.

(8) Liu, H., Zhang, Z., and Linhardt, R. J. (2009) Lessons learned from the contamination of heparin. *Nat. Prod. Rep. 26*, 313−321.

(9) DeAngelis, P. L. (2012) Glycosaminoglycan polysaccharide biosynthesis and production: Today and tomorrow. *Appl. Microbiol. Biotechnol. 94*, 295−305.

(10) Sugahara, K., Mikami, T., Uyama, T., Mizuguchi, S., Nomura, K., and Kitagawa, H. (2003) Recent advances in the structural biology of chondroitin sulfate and dermatan sulfate. *Curr. Opin. Struct. Biol. 13*, 612−620.

(11) Wantanabe, H., Yamada, Y., and Kimata, K. (1998) Roles of aggrecan, a large chondroitin sulfate proteoglycan, in cartilage structure and function. *J. Biochem. 124*, 687−693.

(12) McAlindon, T. E., LaValley, M. P., Gulin, J. P., and Felson, D. T. (2000) Glucosamine and chondroitin for treatment of osteoarthritis − A systematic quality assessment and meta-analysis. *J. Am. Med. Assoc. 283*, 1469−1475.

(13) Linhardt, R. J., and Toida, T. (2004) Role of glycosaminoglycans in cellular communication. *Acc. Chem. Res. 37*, 431−438.
(14) Stringer, S. E., and Gallagher, J. T. (1997) Specific binding of the chemokine platelet factor 4 to heparan sulfate. *J. Biol. Chem. 272*, 20508−20514.
(15) Spillman, D., Witt, D., and Lindahl, U. (1998) Defining the interleukin-8 binding domain of heparan sulfate. *J. Biol. Chem. 273*, 15487−15493.
(16) Saphire, A. C. S., Bobardt, M. D., and Gallay, P. A. (1999) Host cyclophilin A mediates HIV-1 attachment to target cells via haparans. *EMBO J. 18*, 6771−6785.
(17) Pye, D. A., Vives, R. R., Turnbull, J. E., Hyde, P., and Gallagher, J. T. (1998) Heparan sulfate oligosaccharides require 6-*O*-sulfation for promotion of basic fibroblast growth factor mitogenic activity. *J. Biol. Chem. 273*, 22936−22942.
(18) Atha, D. H., Stephans, A. W., and Rosenberg, R. D. (1984) Evaluation of critical groups required for the binding of heparin to antithrombin. *Proc. Natl. Acad. Sci. U.S.A. 81*, 1030−1034.
(19) Jordan, R. E., Oosta, G. M., Gardner, W. T., and Rosenberg, R. D. (1980) The kinetics of hemostatic enzyme-antithrombin interactions in the presences of low molecular weight heparin. *J. Biol. Chem. 255*, 10081−10090.
(20) Lincoln, J., Lange, A. W., and Yutzey, K. E. (2006) Heart and bones: Shared regulatory mechanisms in heart valve, cartilage tendon, and bone development. *Dev. Biol. 294*, 292−302.
(21) Zhang, F., Zhang, Z., Lin, X., Beenken, A., Eliseenkova, A. V., Mohammadi, M., and Linhardt, R. J. (2009) Compositional analysis of heparin/heparan sulfate interacting with fibroblast growth factor·fibroblast growth factor receptor complexes. *Biochemistry 48*, 8379−8386.
(22) Ornitz, D. M., and Itoh, N. (2001) Fibroblast growth factors. *Genome Biol. 3*, 3005−3012.
(23) Powers, C. J., McLeskey, S. W., and Wellstein, A. (2000) Fibroblast growth factors, their receptors and signaling. *Endocr.-Relat. Cancer 7*, 165−197.
(24) Ornitz, D. M., Xu, J., Colvin, J. S., McEwen, D. G., MacArthur, C. A., Coulier, F., Gao, G., and Goldfarb, M. (1996) Receptor specificity of the fibroblast growth factor family. *J. Biol. Chem. 271*, 15292−15297.
(25) Zhang, X., Ibrahimi, O. A., Olsen, S. K., Umemori, H., Mohammadi, M., and Ornitz, D. M. (2006) Receptor specificity of the fibroblast growth factor family. *J. Biol. Chem. 281*, 15694−15700.
(26) Mohammadi, M., Olsen, S. K., and Ibrahimi, O. A. (2005) Structural basis for fibroblast growth factor receptor activation. *Cytokine Growth Factor Rev. 16*, 107−137.
(27) Obrahimi, O. A., Zhang, F., Lang Hrstka, S. C., Mohammadi, M., and Linhardt, R. J. (2004) Kinetic model for FGF, FGFR, and proteoglycan signal transduction complex assembly. *Biochemistry 43*, 4724−4730.
(28) Asada, M., Shinomiya, M., Suzuki, M., Honda, E., Sugimoto, R., Ikekita, M., and Imamura, T. (2009) Glycosaminoglycan affinity of the complete fibroblast growth factor family. *Biochem. Biophys. Acta 1790*, 40−48.
(29) Walker, A., Turnbull, J. E., and Gallagher, J. T. (1994) Specific heparan sulfate saccharides mediate the activity of basic fibroblast growth factor. *J. Biol. Chem. 269*, 931−935.
(30) Luo, Y., Lu, W., Mohamedali, K. A., Jang, J. H., Jones, R. B., Gabriel, J. L., Kan, M., and McKeehan, W. L. (1998) The glycine box: A determinant of specificity for fibroblast growth factor. *Biochemistry 37*, 16506−16515.
(31) Ashikari-Hada, S., Habuchi, H., Kariya, Y., Itoh, N., Reddi, A. H., and Kimata, K. (2004) Characterization of growth factor-binding structure in heparin/heparan sulfate using an octasaccharide library. *J. Biol. Chem. 279*, 12346−12354.
(32) Ornitz, D. M., Herr, A. B., Nilsson, M., Westman, J., Svahn, C. M., and Waksman, G. (1995) FGF binding and FGF receptor activation by synthetic heparan-derived di- and trisaccharides. *Science 21*, 432−436.
(33) Ishihara, M., Shaklee, P. N., Yang, Z., Liang, W., Wei, Z., Stack, R. J., and Holme, K. (1994) Structural features in heparin which modulate specific biological activities mediated by basic fibroblast growth factor. *Glycobiology 4*, 451−458.
(34) Guimond, S. E., and Turnbull, J. E. (1999) Fibroblast growth factor receptor signaling is dictated by specific heparan sulfate saccharide. *Curr. Biol. 9*, 1343−1346.
(35) Lee, M. Y., Kumar, R. A., Sukumaran, S. M., Hogg, M. G., Clark, D. S., and Dordick, J. S. (2008) Three-dimensional cellular microarray for high-throughput toxicology assays. *Proc. Natl. Acad. Sci. U.S.A. 105*, 59−63.
(36) Fernandes, T. G., Kwon, S. J., Lee, M. Y., Clark, D. S., Cabral, J. M. S., and Dordick, J. S. (2008) On-chip, cell-based microarray immunofluorescence assay for high-throughput analysis of target proteins. *Anal. Chem. 80*, 6633−6639.
(37) Fernandes, T. G., Kwon, S. J., Bale, S. S., Lee, M. Y., Diogo, M. M., Clark, D. S., Cabral, J. M. S., and Dordick, J. S. (2010) Three-dimensional cell culture microarray for high-throughput studies of stem cell fate. *Biotechnol. Bioeng. 106*, 106−118.
(38) Puvirajesinghe, T. M., Ahmed, Y. A., Powell, A. K., Fernig, D. G., Guimond, S. E., and Turnbull, J. E. (2012) Array-based functional screening of glycans. *Chem. Biol. 19*, 553−558.
(39) Wang, Z., Ly, M., Zhang, F., Zhong, W., Suen, A., Dordick, J. S., and Linhardt, R. J. (2010) *E. coli* K5 fermentation and the preparation of heparosan, a bioengineered heparin precursor. *Biotechnol. Bioeng. 107*, 968−977.
(40) Wang, Z., Yang, B., Zhang, Z., Ly, M., Takieddin, M., Mousa, S., Liu, J., Dordick, J. S., and Linhardt, R. J. (2011) Control of the heparosan N-deacetylation leads to an improved bioengineered heparin. *Appl. Microbiol. Biotechnol. 91*, 91−99.
(41) Yates, E. A., Santini, F., Guerrini, M., Naggi, A., Torri, G., and Casu, B. (1996) ^{1}H and ^{13}C NMR spectral assignments of the major sequences of twelve systematically modified heparin derivatives. *Carbohydr. Res. 294*, 15−27.
(42) Li, K., Bethea, H. N., and Liu, J. (2010) Using engineered 2-*O*-sulfotransferase to determine the activity of heparan sulfate C_5-epimerase and its mutants. *J. Biol. Chem. 285*, 11106−11113.
(43) Ornitz, D. M., Yayon, A., Flanagan, J. G., Svahn, C. M., Levi, E., and Leder, P. (1992) Heparin is required for cell-free binding of basic fibroblast growth factor to a soluble receptor and for mitogenesis in whole cells. *Mol. Cell. Biol. 12*, 240−247.
(44) Zhang, Z., Xie, J., Liu, H., Liu, J., and Linhardt, R. J. (2009) Quantification of heparan sulfate disaccharides using ion-pairing reversed-phase microflow high-performance liquid chromatography with electrospray ionization trap mass spectrometry. *Anal. Chem. 81*, 4349−4355.
(45) Zhang, F., Yang, B., Ly, M., Solakyildirim, K., Xiao, Z., Wang, Z., Beaudet, J. M., Torelli, A. Y., Dordick, J. S., and Linhardt, R. J. (2011) Structural characterization of heparins from different commercial sources. *Anal. Bioanal. Chem. 401*, 2793−2803.
(46) Xu, Y., Masuko, S., Takieddin, M., Xu, H., Liu, R., Jing, J., Mousa, S., Linhardt, R. J., and Liu, J. (2011) Chemoenzymatic synthesis of structurally homogeneous ultra-low molecular weight heparins. *Science 334*, 498−501.